DISTRIBUTION OF STARSPOTS ON COOL STARS

A model based on the dynamics of magnetic flux tubes

M. SCHÜSSLER

Kiepenheuer-Institut
Schöneckstr. 6, D-79104 Freiburg, Germany
msch@kis.uni-freiburg.de

Abstract. A theoretical study of storage, instability and rise of magnetic flux tubes in the outer convection zone of a cool star is presented. Special emphasis is laid on their emergence latitudes at the surface of magnetically active stars. We apply the 'solar paradigm' and assume toroidal magnetic flux tubes to be stored in force equilibrium within the overshoot layer underneath the convection zone. A non-axisymmetric (undulatory) instability leads to the formation of flux loops, which rise through the convection zone and emerge at the surface to form bipolar magnetic regions and starspots. Our approach combines the analytical determination of the linear stability properties of flux tubes with numerical simulations of the nonlinear evolution of the instability and the rise of magnetic flux tubes through the convection zone. It is found that for sufficiently rapidly rotating stars the magnetic flux emerges at high latitudes since the Coriolis force leads to a poleward deflection of rising flux loops. The latitude distribution of the emerging flux is determined for a number of stellar models along the evolutionary sequence of a star with one solar mass, from the pre-main sequence evolution up to the giant phase. Rapid rotation and deep convection zones favour flux emergence in high latitudes. Starspots right at the stellar (rotational) poles form either directly by flux eruption from small stellar cores (as for T Tauri stars or giants) or by a poleward slip of the sub-surface part of the flux tube after flux emergence in mid latitudes. The latter process explains the simultaneous existence of polar spots and spots at intermediate latitudes as observed on some stars.

K. G. Strassmeier and J. L. Linsky (eds.), Stellar Surface Structure, 269–287.

1. Sunspots and starspots

It is well known that sunspots appear within a latitude band of about $\pm 30°$ from the solar equator. So it came as a surprise when most of the stars observed with the Doppler imaging technique (Vogt & Penrod, 1983) revealed spots in high latitudes. Many of these stars actually show dark polar caps covered with magnetic fields (e.g. Donati et al., 1992).

What causes the different latitude distributions and the apparent failure of the 'solar paradigm' ? In order to answer this question we have to consider the differences between the Sun and the observed active stars. First, the Doppler-imaged stars have larger *rotation rates* than the Sun; their angular velocities are typically a factor 10 larger than the solar value. This is due to a two-fold selection effect: on the one hand, magnetic activity increases with the rotation rate, so that rapid rotators show more magnetic flux at their surfaces; on the other hand, the Doppler-imaging technique itself does only work for sufficiently rapid rotation. The other important difference between the Sun and most of the imaged stars concerns their *evolutionary status:* most of the spotted stars are (sub-)giants in close binary systems or pre-main-sequence stars. They have deeper outer convection zones than the Sun, which may affect the generation and dynamics of magnetic fields.

It is conceivable that the differences between the Sun and the Doppler-imaged stars lead to a different mechanism or operational mode of the hydromagnetic dynamo that is held responsible for the generation of the magnetic field. In view of our poor understanding of the dynamo (even for the solar case) we could not proceed much further if we were to follow this approach. However, we shall argue in what follows that we can understand the latitude distribution of starspots by considering the *stability and dynamics of magnetic flux tubes* alone, without having to bother with the details of the dynamo process. The success of this approach in explaining the observations confirms the validity of the solar paradigm for magnetically active stars.

2. The solar paradigm

This section gives a brief summary of flux tube dynamics in the Sun and the basic model for the origin of solar active regions. More details can be found in Schüssler et al. (1994), Caligari et al. (1995), and Schüssler (1996).

The observed properties of sunspot groups indicate that they originate from the emergence of coherent magnetic structures which are generated and stored in a from a source region of well-ordered toroidal magnetic flux in the solar interior (e.g., Zwaan, 1992; Zwaan & Harvey, 1994). We describe these structures as *magnetic flux tubes,* i.e., bundles of magnetic field lines that are separated from their non-magnetic environment by a tangential

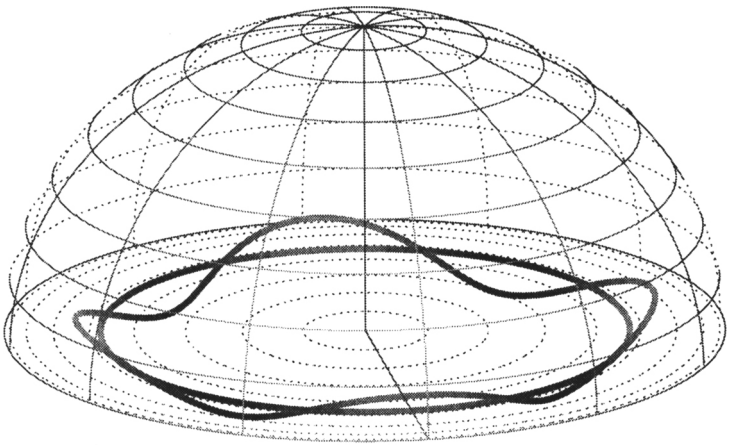

Figure 1. Undulatory instability of a toroidal flux tube. In the case sketched here, the initial flux ring is perturbed by a displacement of azimuthal wavenumber $m = 4$. A downflow of plasma from the crests into the troughs lets the summits rise while the valleys sink.

discontinuity with a surface current. Flux tubes form through magnetic flux expulsion by convective flows (Proctor & Weiss, 1982) or the magnetic Rayleigh-Taylor instability (e.g., Cattaneo & Hughes, 1988).

Magnetic and convective buoyancy (Parker, 1975; Moreno-Insertis, 1983) prevent strong magnetic flux tubes from being stored within the superadiabatically stratified convection zone for a sufficiently long time to be amplified in the course of the dynamo process with its 11-year time scale. Therefore, a region of *convective overshoot* below the convection zone proper has been proposed as the site of the dynamo process (Spiegel & Weiss, 1980): the stable stratification acts against magnetic buoyancy while turbulence and flows provide necessary ingredients for the dynamo. The helioseismological discovery of a shear layer of strong radial differential rotation at the bottom of the convection zone (Schou et al., 1994, Tomczyck et al., 1995) gave support to this conjecture.

The following gives a sketch of the consistent picture of the storage, instability, and rise of magnetic flux tubes that has emerged through linear stability analysis and nonlinear numerical simulations. It is assumed that the dynamo generates toroidal magnetic flux tubes, which are stored in force equilibrium within the overshoot layer (Moreno-Insertis et al., 1992). They are continuously intensified by differential rotation until the field strength exceeds the threshold for the onset of the *undulatory instability* (Spruit

& van Ballegooijen, 1982; Ferriz-Mas & Schüssler, 1993, 1994, 1996). This instability is akin to the Parker instability and in most cases sets in for non-axisymmetyric perturbations as sketched in Fig. 1. A downflow of plasma along the field lines within the flux tube leads to an upward buoyancy force acting on the outward displaced parts and a downward force on the troughs, so that the perturbation grows. As a consequence, flux loops form, rise through the convection zone, and finally emerge at the surface to form sunspots. The sinking parts of the tube reach a new equilibrium at the bottom of the overshoot region and effectively 'anchor' the erupted loop.

Applied to the overshoot layer of the Sun, the linear stability analysis predicts that undulatory instability sets in for field strengths of the order of 10^5 G in the storage region. Numerical simulations show that the dynamical evolution of flux tube in this range of field strengths is in accordance with the observed properties of sunspot groups. This applies in particular to their eruption in low latitudes (Choudhuri & Gilman, 1987), their coherence and lifetime (Moreno-Insertis, 1992), the tilt angle with respect to the direction of rotation (D'Silva & Choudhuri, 1993), and their characteristic asymmetry and proper motions (Caligari et al., 1995).

The value of 10^5 G is an order of magnitude larger than the equipartition field, i.e. the field strength for which the magnetic energy density equals the kinetic energy density of the convective motions. This raises questions concerning the origin of such strong fields, which cannot be discussed here. The interested reader is referred to Schüssler (1993, 1996), Ferriz-Mas et al. (1994), and Moreno-Insertis et al. (1995).

3. Why do rapid rotator have polar spots ?

In order to understand the observed preference of starspots to occur in high latitudes we have to consider the various forces acting on a magnetic flux tube in a stellar convection zone. If the diameter of the flux tube is small compared to all other relevant length scales (scale heights, wavelengths, radius of curvature, etc.) the *thin flux tube approximation* can be employed, a quasi-1D description that greatly simplifies the mathematical treatment (Spruit, 1981, Ferriz-Mas & Schüssler, 1993). The forces that are most important for the dynamics of a magnetic flux tube are the *buoyancy force*, the *magnetic curvature force* (if the tube is non-straight), the *Coriolis force* (due to rotation), and the *drag force* (for motion relative to the surrounding plasma). Figure 2 sketches the geometry of these forces for an axisymmetric toroidal flux tube (a flux ring). The drag force (not shown) is always anti-parallel to the velocity of the tube relative to the ambient gas, the buoyancy force (anti-)parallel to gravity, while the curvature and rotational (Coriolis and centrifugal) forces are perpendicular to the axis of the star.

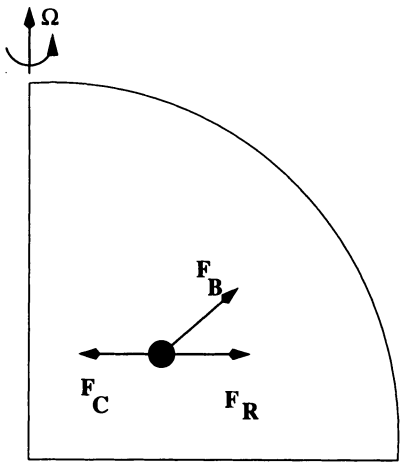

Figure 2. Forces on an axisymmetric flux tube. The buoyancy force (F_B), rotationally induced force (F_R), and magnetic curvature force (F_C) are shown in a meridional plane. The cross section of the flux tube is indicated by the black disk. While F_R and F_C are perpendicular to the axis of rotation, the buoyancy force is (anti)parallel to the radial direction of gravity.

Choudhuri & Gilman (1987) first realized that rotation may have a strong influence on axisymmetric flux tubes rising due to buoyancy: the Coriolis force deflects the flux rings to high latitudes unless their initial field strength is larger than about 10^5 G (in the case of the Sun). The following simple example illustrates the effect (see Fig. 3). Assume a flux ring in the equatorial plane, which has been set into an expanding motion with velocity u_r (by the action of a buoyancy force, for example). In a rotating system, this motion causes a Coriolis force which drives a flow u_ϕ along the tube and against the direction of rotation, reflecting the conservation of angular momentum. This velocity, in turn, causes an *inward* directed Coriolis force, which acts as a restoring force with respect to the expansion of the flux ring. As a consequence, the radial motion of the flux ring is transformed into an *inertial oscillation* with a period 2Ω, whose amplitude depends on the strength of the initial buoyancy force. If we are outside the equatorial plane, however, the Coriolis force affects only the component of the buoyancy force perpendicular to the axis of rotation (see Fig. 2); the trajectory of the flux ring then becomes the superposition of an inertial oscillation in the plane perpendicular to the axis of rotation and a rise parallel to the axis. If the Coriolis force dominates (i.e., if the rise time is longer than the period of the inertial oscillation) this leads to the eruption of magnetic flux in high latitudes.

Schüssler and Solanki (1992) put forward the conjecture that the polar spots observed on rapidly rotating, active stars are due to this effect of the

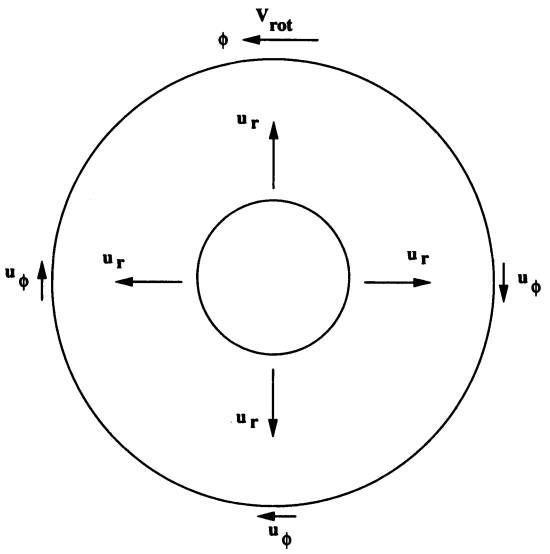

Figure 3. Effect of rotation on an expanding flux ring, which is seen from above along the axis of rotation. Due to angular momentum conservation, the expansion motion u_r causes a flow u_ϕ against the direction of rotation. This leads to an *inward* directed Coriolis force, which acts against the further expansion of the flux ring.

Coriolis force on rising flux tubes. To order of magnitude, they estimated the ratio of the Coriolis force (F_R) to the buoyancy force (F_B)

$$\frac{|F_{\rm R}|}{|F_{\rm B}|} \simeq \frac{2\,\varrho\, v_{\rm rise}\,\Omega}{B^2/8\pi H} \propto \frac{\Omega}{B}, \tag{1}$$

where B is the magnetic field strength, H the pressure scale height, ϱ the density, and Ω the stellar rotation rate. The rise velocity, $v_{\rm rise}$, has been assumed here to be of the order of the Alfvén velocity, $v_A = B/(4\pi\rho)^{1/2}$ (Parker, 1975). For a given rotation rate, the Coriolis force dominates and the flux tubes are deflected poleward and emerge in high latitudes if their field strength (in the deep parts of the stellar convection zone) is not too large, viz.

$$B < B_{\rm m} \equiv 8\,H\,\Omega\sqrt{\pi\,\varrho}\,. \tag{2}$$

Otherwise, the buoyancy force dominates and the flux tubes erupt more or less radially, thus allowing for starspots and stellar active regions in low latitudes.

The initial field strength of erupting flux tubes is determined by the stability criteria with respect to the undulatory instability. Since rotation exerts a stabilizing influence, the critical field strength for instability increases

https://doi.org/10.1017/S0074180900083297 Published online by Cambridge University Press

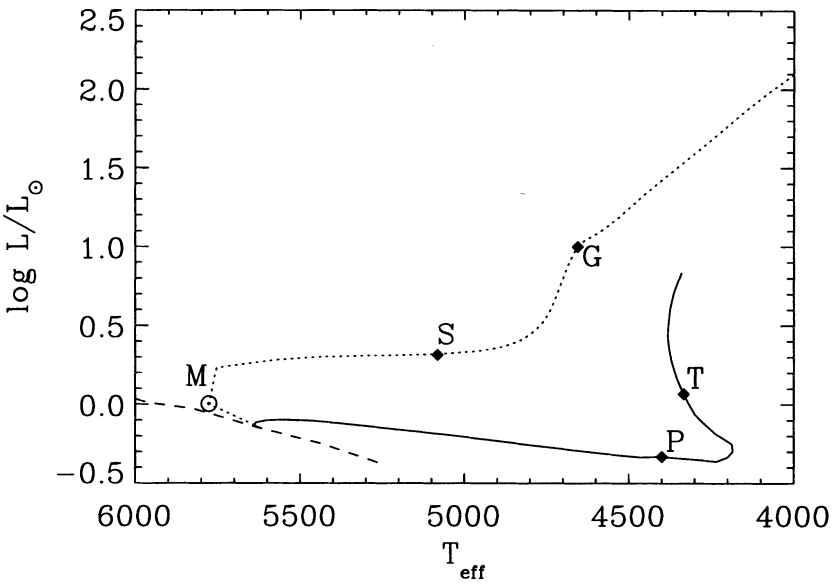

Figure 4. Evolutionary path of a 1 $M_\odot$ star in the Hertzsprung-Russell diagram (full line: pre-main-sequence evolution, dotted line: post-main-sequence. The models considered here are indicated. The corresponding part of the zero-age main sequence is denoted by the dashed line.

with Ω, so that we cannot say beforehand how the ratio Ω/B changes as a function of angular velocity. Moreover, the estimate in equation (1) does not fully take into account the effect stellar stratification (superadiabaticity, in particular) and depth of the convection zone on the dynamics of flux tubes and their emergence latitude. Consequently, a detailed study of the linear stability criteria (to determine B) and the nonlinear evolution of the instability by numerical simulation (to determine the actual emergence latitudes) for realistic stellar models is necessary in order to make quantitative statements about the expected latitude distribution of starspots on the basis of this approach. In the following section results from such a study are shown; a more detailed presentation will be given by Schüssler et al. (1996a,b).

4. Spotty evolution of a 1 $M_\odot$ star

4.1. STELLAR MODELS

A number of stellar models from an evolutionary sequence of a star with one solar mass between the Hayashi track and the giant phase have been analyzed. Fig. 1 shows the evolutionary path in the Hertzsprung-Russell

https://doi.org/10.1017/S0074180900083297 Published online by Cambridge University Press

diagram, where the models considered are indicated by letters. They represent five distinct phases of this evolution: model 'T' on the lower part of the Hayashi track has already developed a small radiative core and may represent a T Tauri star; model 'P' is a pre-main-sequence star in the middle of its transition from the Hayashi track onto the the zero-age main sequence; the Sun serves as a prototype main sequence star (model 'M'), while models 'S' and 'G' represent the subgiant and the giant phase, respectively. Some properties of these models are listed in Table 1. Models T, P, and M have been provided by M. Stix (see Skaley & Stix, 1990), who introduced a non-local description of the convective energy transport according to the method proposed by Shaviv & Salpeter (1973). This leads to a subadiabatically stratified overshoot layer below the outer convection zone of the stellar model, which is the assumed location for the generation and storage of magnetic flux tubes. The post-main-sequence models S and G have been calculated by D. Schaerer (Geneva Observatory; see Schaller et al. 1992).

Model	Age (yr)	$R/R_\odot$	$T_{\rm eff}$ (K)	r_0/R	d (Mm)	δ
T	$2.1 \cdot 10^6$	1.9	4330	0.16	117	$-2.9 \cdot 10^{-8}$
P	$1.1 \cdot 10^7$	1.2	4400	0.54	22	$-5.8 \cdot 10^{-7}$
M	$4.6 \cdot 10^9$	1.0	5780	0.72	10	$-2.6 \cdot 10^{-6}$
S	$1.2 \cdot 10^{10}$	1.9	5100	0.48	33	$-7.6 \cdot 10^{-7}$
G	$1.3 \cdot 10^{10}$	4.8	4690	0.10	44	$-4.7 \cdot 10^{-6}$

Table 1. Properties of the stellar models. The given quantities are the age, the radius in units of the present solar radius ($R/R_\odot$), the effective temperature ($T_{\rm eff}$), the fractional radius of the bottom of the overshoot region (r_0/R), the thickness of the overshoot layer (d), and the superadiabaticity $\delta \equiv \nabla - \nabla_{\rm ad}$ near the bottom of the overshoot layer.

4.2. ESTIMATE AND PROCEDURE

Schüssler and Solanki (1992) have estimated the minimum field strength, $B_{\rm m}$, for the dominance of the buoyancy force (and radial emergence of flux tubes) on the basis of equation (2). In terms of values for the present Sun, $B_{\rm m}$ is given by

$$B_{\rm m} \simeq 10^5 \left(\frac{H}{H_\odot}\right) \left(\frac{\varrho}{\varrho_\odot}\right)^{1/2} \left(\frac{\Omega}{\Omega_\odot}\right) \ {\rm G} \qquad (3)$$

For the models considered here, the factor arising from the stellar structure is given in Table 2.

https://doi.org/10.1017/S0074180900083297 Published online by Cambridge University Press

Model	ϱ [g·cm^{-3}]	H [cm]	$(H/H_\odot)(\varrho/\varrho_\odot)^{1/2}$
T	1.2	$3.9 \cdot 10^{10}$	18.5
P	1.6	$1.1 \cdot 10^{10}$	6.1
M	0.2	$5.6 \cdot 10^{9}$	1.0
S	0.3	$1.5 \cdot 10^{10}$	3.3
G	0.2	$2.0 \cdot 10^{10}$	3.6

Table 2. Influence of stellar structure on the relation of Coriolis and buoyancy force. The factor in the estimate given in equation (3) is given for the stellar models considered.

We see from Table 2 that the estimate given in equation (3) predicts the minimal influence of the Coriolis force for the present Sun: for any given Ω, the field strength required for a dominance of the buoyancy force over the Coriolis effect is smallest. Consequently, within our sample of stellar models we expect the weakest rotational influence on rising flux tubes for the model of the present Sun (model M).

In order to determine the emergence latitudes of flux tubes we have carried out the following procedure (for a more detailed discussion see Schüssler et al., 1996a). Axisymmetric flux tubes are assumed to be stored in mechanical force equilibrium in the overshoot layer below the outer stellar convection zone. From the linear stability analysis we determine the magnetic field strength which corresponds to a certain growth time of the instability, typically a value of one year. The resulting field strength depends on the stellar model, the original latitude of the flux ring, and on the rotation rate of the star. For these parameters we then perform the numerical simulation of the nonlinear development of the instability and follow the erupting loop(s) nearly up to the stellar surface until the thin flux tube approximation breaks down and the simulation has to be terminated. The equations and the numerical procedure underlying the simulation have been described by Caligari et al. (1995).

4.3. LATITUDE DISTRIBUTION OF EMERGING FLUX

We first give the results for the model of the present Sun (model M) as a prototype cool main-sequence star. On the left-hand side of Fig. 5 stability diagrams resulting from the linear stability analysis are given for three values of the rotation rate, namely $\Omega_\odot = 2.7 \cdot 10^{-6}$ s^{-1}, $10\,\Omega_\odot$, and $60\,\Omega_\odot$, respectively. This corresponds to rotation periods of 27 days, 2.7 days, and 0.45 days, respectively. We assume rigid rotation in all cases. This

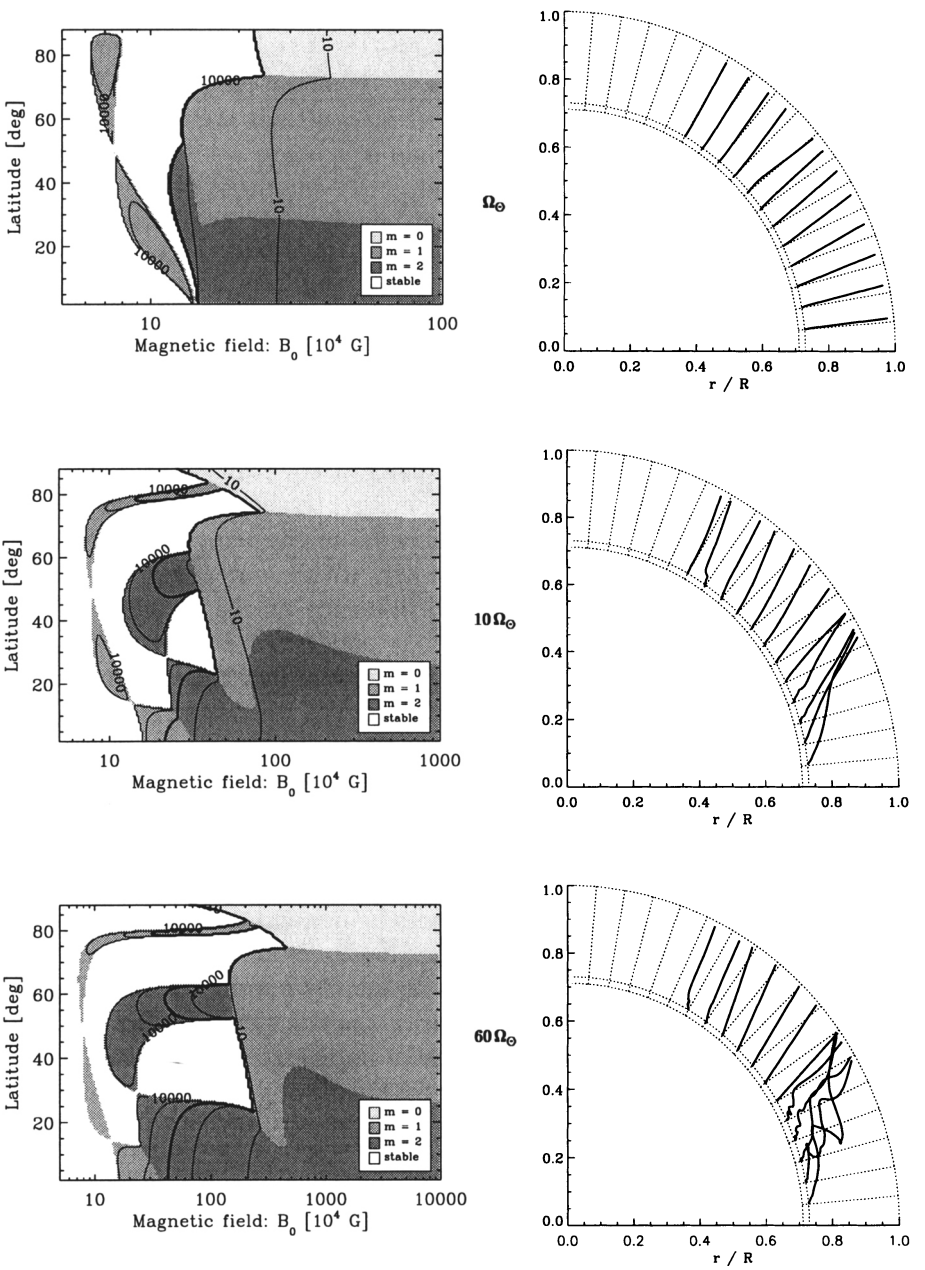

Figure 5. Stability diagrams (*left*) and meridional projection of trajectories of rising flux loops (*right*) for model M (present Sun) and three different rotation rates: $\Omega_\odot$ *(top)*, $10\,\Omega_\odot$ *(middle)*, and $60\,\Omega_\odot$ *(bottom)*. The trajectories are drawn from the moment when the top of the rising flux loop leaves the overshoot region (indicated by the dotted quarter-circles). While the flux tubes erupt nearly radially for $\Omega_\odot$, higher rotation rates lead to an 'equatorial gap' devoid of emerging magnetic flux.

https://doi.org/10.1017/S0074180900083297 Published online by Cambridge University Press

seems justified since the differential rotation of the present Sun does not significantly influence the properties of rising flux loops (Caligari et al., 1995); for more rapidly rotating stars an even smaller amount of differential rotation in the convection zone is indicated by observations (e.g., Hall, 1990) and also predicted by theoretical models (e.g., Kitchatinov & Rüdiger, 1995). The stability properties are indicated in the (B_0, λ_0)-plane, where B_0 is the field strength and λ_0 is the latitude of the equilibrium flux tube. Note that the horizontal scale (magnetic field) is not the same for the three stability diagrams in Fig. 5. White regions in the stability diagrams denote stable flux tubes while the shaded regions indicate instability. The contour lines give the linear growth time of the instability; the thick contour line corresponds to a growth time of 300 days. The degree of shading indicates the azimuthal wave number of the unstable mode with the largest growth rate. For $m \neq 0$ the instability leads to the formation of m rising flux loops that eventually emerge at the surface and form bipolar magnetic regions. The case $m = 0$ corresponds to the axisymmetric mode, i.e., the flux tube maintains the form of a toroidal flux ring during its rise. Presumably such a flux ring forms loops at some later stage of its eruption, either due to nonlinear excitation of non-axisymmetric modes, local instability near the surface, or caused by the influence of convective velocities on the weakening flux tube.

A more detailed discussion of the stability diagrams can be found in Schüssler et al. (1996). Here we only note the following properties: (1) instability sets in for field strengths above 10^5 G; (2) the field strength required for significant growth of the instability (growth times of a year or less) increases with the rotation rate. However, this increase is not sufficient to prevent the dominance of the Coriolis force for fast rotation. We have followed the evolution of unstable flux rings initially located at latitudes between 5° and 60°. The panels on the right-hand side of Fig. 5 show the result of the nonlinear simulations. Since we are mainly interested in the amount of poleward deflection and in the emergence latitudes, it is sufficient to show the trajectories of the rising loop summits in a meridional projection. While for $\Omega = \Omega_\odot$ the flux tubes emerge almost radially, there is a significant poleward deflection for the higher rotation rate and an 'equatorial gap' up to about 30° latitude, which is devoid of erupting magnetic flux, appears.

The corresponding results for the pre-main-sequence star (model P) are given in Fig. 6. The stability diagrams show an 'island of stability', a range of field strength in mid latitudes for which the corresponding flux tubes are stable. Instability with significant growth rates in this latitude range requires much larger field strengths than in high or low latitudes. The island actually represents a stable transition between two different regimes of

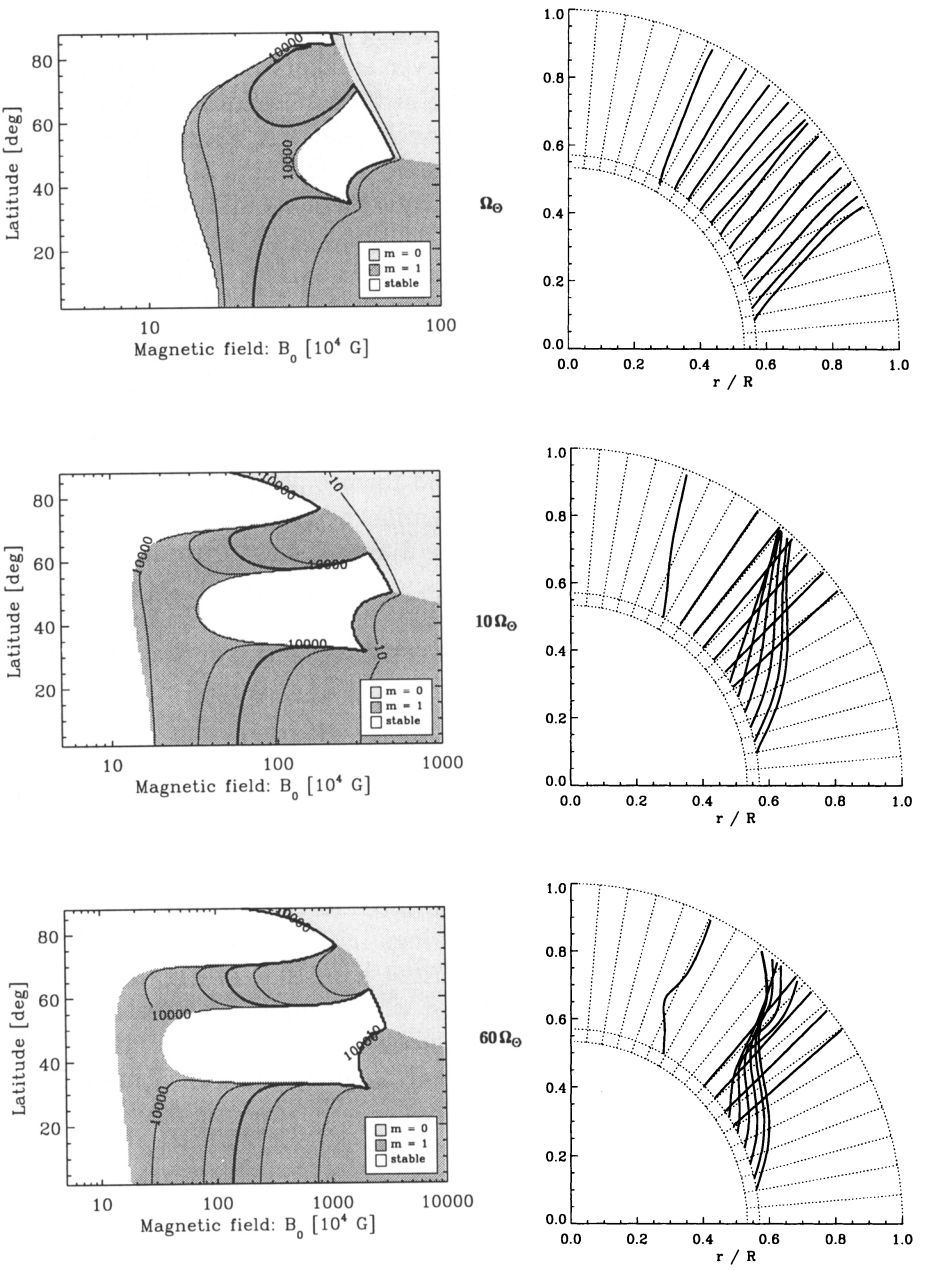

Figure 6. Stability diagrams (*left*) and meridional projection of trajectories of rising flux loops (*right*) for model P (pre-main-sequence star). The rotational deflection is significant even for solar rotation. For larger angular velocities, the 'island of stability' leads to nearly radial emergence in mid latitudes, while flux tubes originating at low latitudes rise nearly parallel to the rotation axis.

https://doi.org/10.1017/S0074180900083297 Published online by Cambridge University Press

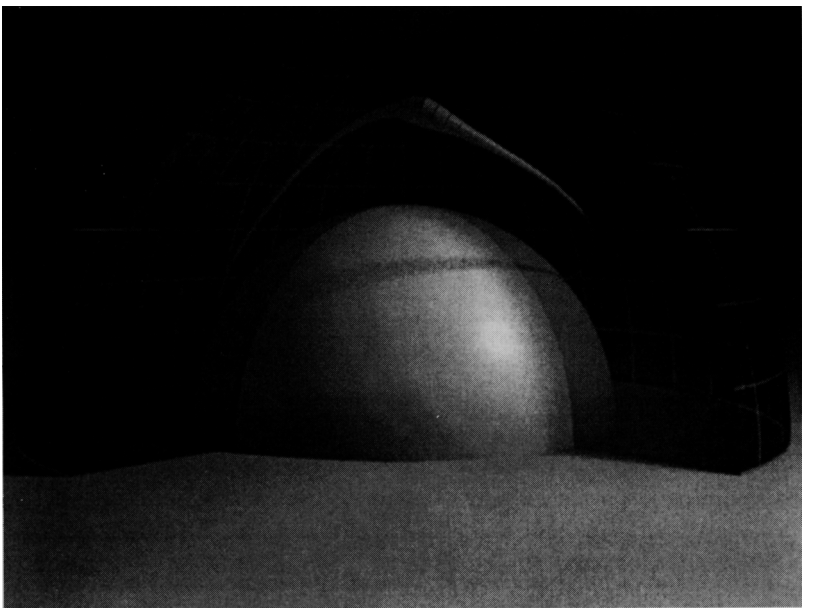

Figure 7. Three-dimensional view of an unstable flux tube in model P, shortly before erupting at the surface. The northern hemisphere of the star is represented; rotation ($\Omega = 10\,\Omega_\odot$) is counter-clockwise with respect to the vertical axis. The transparent outer half-sphere corresponds to the stellar surface while the inner half-sphere indicates the bottom of the convection zone.

instability, one of which is only weakly dependent on rotation. As the other regime moves towards higher field strength for increasing angular velocity, the transition region of stable flux tube equilibria (the island) widens. The trajectories of rising flux tubes for model P in Fig. 6 show that the deeper convection zone of this star (corresponding to larger scale height and higher density in its deep parts) in comparison to model M leads to a significant poleward deflection of the rising loops even for $\Omega = \Omega_\odot$. For larger angular velocity, flux tubes from the latitude range of the stability island have sufficiently large field strength to emerge nearly radially while flux loops originating in lower latitudes are strongly deflected to higher latitudes. As a consequence, we expect such stars to show activity in mid latitudes, irrespective of their rotation rates. This result could well be related to the starspots observed at intermediate latitudes of rapidly rotating pre-main-sequence stars.

A three-dimensional view of a flux loop rising through the convection zone of model P is given in Fig. 7, which shows the final state of a numerical simulation. The corresponding initial flux ring was located in the overshoot layer at a latitude of 15°. The assumed rotation rate is $10\,\Omega_\odot$. The outer (transparent) half-sphere corresponds to the stellar surface while

https://doi.org/10.1017/S0074180900083297 Published online by Cambridge University Press

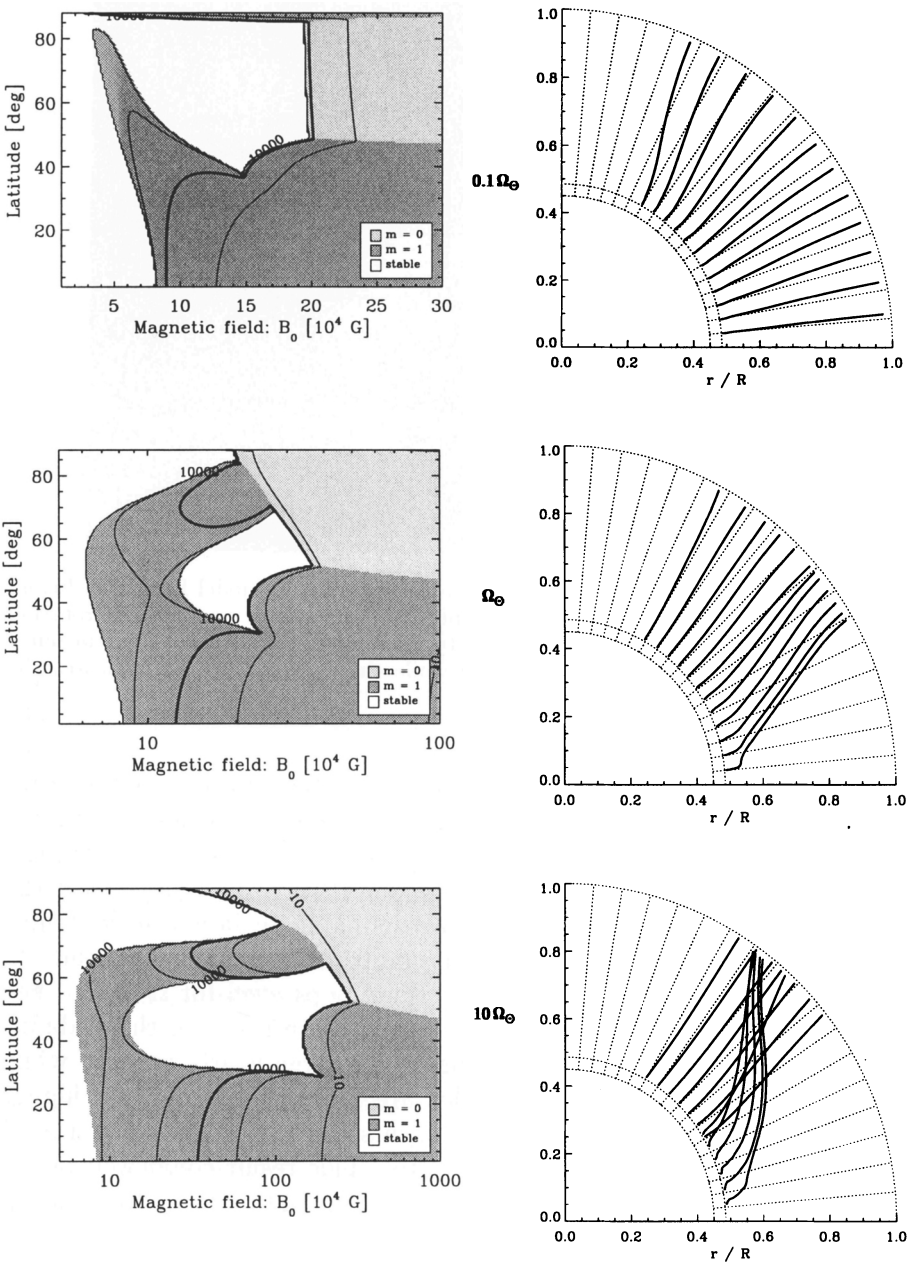

Figure 8. Stability diagrams (*left)* and meridional projection of trajectories of rising flux loops (*right)* for model S (subgiant). The rotational influence be neglected only for very slow rotation ($0.1\,\Omega_\odot$, top panels). Similar to the results for model P, a stability island leads to radially emerging flux loops in mid latitudes for sufficiently large angular velocity.

https://doi.org/10.1017/S0074180900083297 Published online by Cambridge University Press

the inner (opaque) half-sphere indicates the bottom of the convection zone. The azimuthal wavenumber of the instability is $m = 1$, so that one loop has formed and risen through the convection zone. The decreasing external gas pressure leads to a strong expansion of the upper part of the erupting loop, which is easily visible as a 'bulge'. Obviously, the effect of the Coriolis force dominates the dynamics in this case, so that the rising loop has been strongly deflected poleward to emerge at a latitude of 55°. The remaining part of the flux tube is anchored at the bottom of the overshoot layer, nearly at its initial latitude of 15°.

The linear stability and numerical simulaton results for the subgiant (model S) are given in Fig. 8. The rotational influence on the rising loops is even larger than for model P. Only for a rotation rate as low as $0.1\,\Omega_\odot$ (shown in the top panels) the poleward deflection is negligible. For larger rotation rates the results are similar to those of model P: strong poleward deflection and radially rising loops in the latitude range of the 'stability island' (bottom panels).

4.4. POLAR SPOTS

Where are the polar spots ? The results shown so far show strong poleward deflection for large rotation rates but the emergence latitudes extend only to about 60° in latitude. This is due to a simple geometrical constraint: since the maximum effect of the Coriolis force is reached when the flux tube rises parallel to the axis of rotation, the ratio between the radius of the radiative core, r_0, and the radius of the star, R, determines the maximum emergence latitude for flux tubes originating in low latitudes. Consequently, we should expect that model T (T Tauri star) and model G (giant) with their low values of r_0/R (see Table 1) provide the best conditions for truly polar spots. Numerical calculations for the giant model are not available at present, but the results for model T support this conjecture. Fig. 9 shows the stability diagram (upper panel) and the projected trajectories of the crest of rising flux loops for model T.

The stability diagrams show that the axisymmetric mode ($m = 0$) is dominant in the linear phase of the instability, so that the influence of angular momentum conservation and Coriolis force is particularly strong. Moreover, model T has a much larger scale height near the bottom of its convection zone than the other models; this leads to a weaker buoyancy force and so favors the dominance of the Coriolis force (see Table 2). In the simulations shown in Fig. 9 we have assumed that the flux tubes remain axisymmetric during their whole evolution. In reality, however, non-axisymmetric modes will be excited nonlinearly, loops form, and eventually bipolar magnetic regions emerge at the surface.

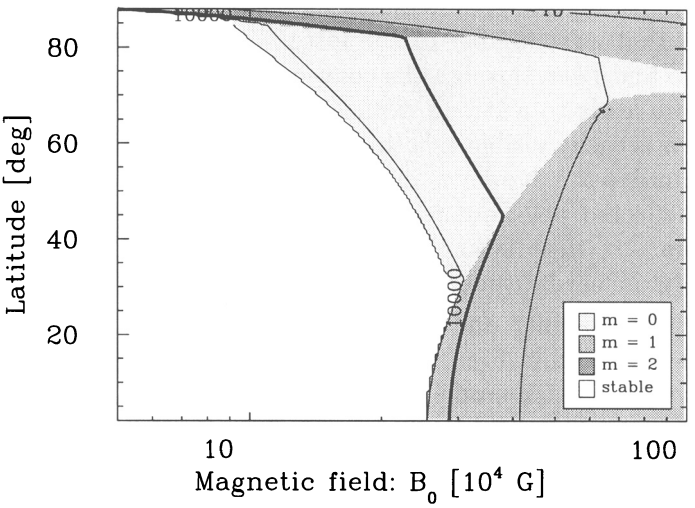

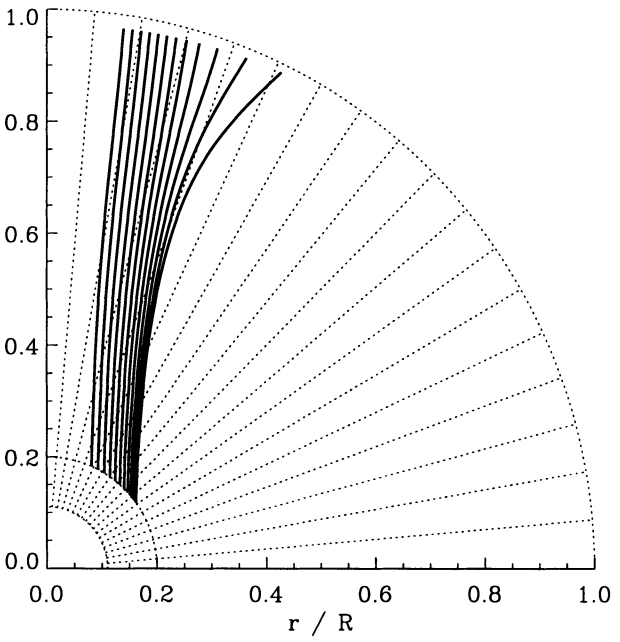

Figure 9. Stability diagram (*upper panel*) and trajectories of rising loops (*lower panel*) for model T (T Tauri star) with $\Omega = \Omega_\odot$. The instability grows fastest for azimuthal wave number $m = 0$. The rotational influence on the rising loops is strong and leads to emergence in the polar regions because of the small relative core radius ($r_0/R = 0.16$).

https://doi.org/10.1017/S0074180900083297 Published online by Cambridge University Press

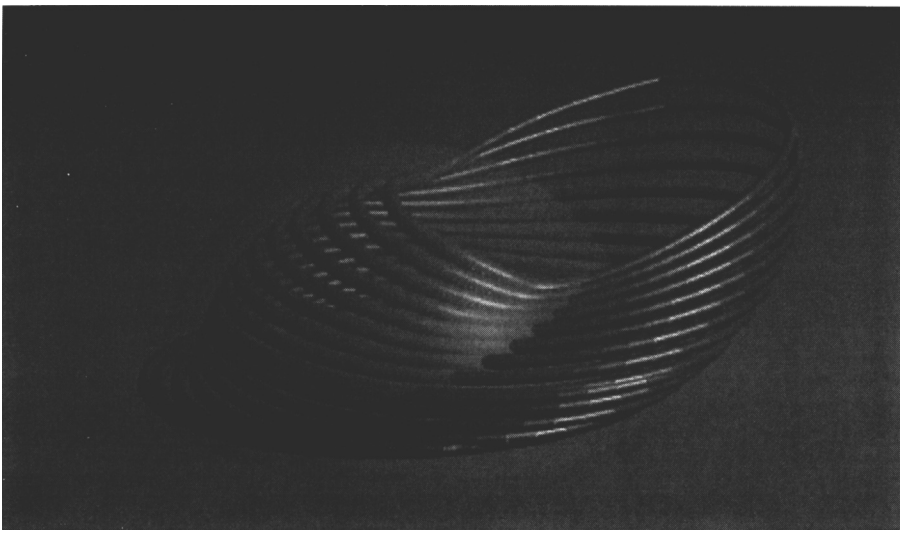

Figure 10. Time evolution of an unstable flux tube in model G. The transparent half-sphere indicates the bottom of the convection zone. The conservation of angular momentum in the rising loop (to the right) slows the flow along the flux tube, which is necessary for the force balance of the part still anchored in the overshoot layer (to the left). As a result, the magnetic tension force is unbalanced and the anchored part slips towards the pole, carrying with it the emerging part.

The results for model T show that we can expect magnetic flux to appear in the polar regions of active stars if they have a sufficiently small radiative core; this applies to very young (T Tauri) stars and also to giants. However, it is well known that many of the stars for which polar spots are observed are *subgiants* in RS CVn binaries. The results for our subgiant model (S) do not show flux emergence near the poles. On the other hand, our simulations apply only the locations of flux *emergence*, not to the possible subsequent evolution and motion of the erupted flux. Meridional circulation might play a role in the redistribution of surface flux, although for the case of the Sun there is no significant effect of meridional flows on sunspots (while the non-spot magnetic fields seem to be affected; see Dikpati & Choudhuri, 1994). From our simulations we have the indication that the sub-surface evolution of the magnetic flux tube after loop emergence can be quite important. For very strong initial fields (as in the 'island' cases) or small stellar core, the force equilibrium in the non-emerged part of the flux tube (see Moreno-Insertis et al., 1992), which is 'anchored' in the overshoot layer, breaks down: angular momentum conservation in the rising loop decelerates the equilibrium flow along the tube and the tension force is no longer balanced.

As a result, the anchored part slips towards the pole like a rubberband on a polished sphere and pulls the emerged loop with itself. Fig. 10 shows an example of this process.

This 'poleward slip' of the anchored part of an erupted flux loop opens an alternative path for the evolution of polar spots on stars with relatively large radiative cores: magnetic flux emerges in mid latitudes and subsequently migrates to the poles to supply the magnetic polar cap, following the motion of the subsurface part of the flux tube. This would explain also the simultaneous existence of truly polar spots and features in lower latitudes. The observed poleward motion of mid-latitude spots observed in the case of HR 1099 (Vogt, these proceedings) is in agreement with this concept.

5. Conclusions

We summarize our conclusions in the following statements:

- The 'solar paradigm' can be successfully utilized to understand the observed latitudes of starspots: the dynamics of rising flux tubes under the influence of buoyancy, Coriolis and magnetic tension forces determines the surface distribution of emerging flux.
- Active stars show high-latitude spots if they are more rapidly rotating or in other evolutionary phases (pre- or post-main-sequence) than the present Sun. This result is in agreement with the estimate given by Schüssler & Solanki (1992).
- For cool main-sequence stars we find a more or less pronounced 'equatorial gap' devoid of emerging magnetic flux, which widens as the rotation rate increases.
- Pre-main sequence stars and subgiants show high-latitude spots (depending on Ω) and flux emergence in mid latitudes (independent of Ω) due to the existence of the stability island. The loss of force balance in the anchored part of the flux tube may cause a 'poleward slip' of the submerged part, which leads to poleward motion of the spots that first emerge in mid latitudes.
- T-Tauri stars and giants with small (relative) core radius develop truly polar spots, even for slow rotation.
- In all cases, the emerging flux loops lead to *bipolar* magnetic regions. Consequently, we expect that starspots have a complex magnetic structure. This applies in particular to the polar spots.

This work will be continued by considering giants, stars with other masses, and close binaries with strong tidal forces.

References

Caligari, P., Moreno-Insertis, F., Schüssler, M. 1995, ApJ, 441, 886
Cattaneo, F., Hughes, D.W. 1988, J. Fluid Mech., 196, 323
Choudhuri, A.R., Gilman, P.A. 1987, ApJ, 316, 788
D'Silva, S., Choudhuri, A.R. 1993, A&A, 272, 621
Dikpati, M., Choudhuri, A.R. 1994, A&A, 291, 975
Donati, J.-F., Brown, S.F., Semel, M., Rees, D.E., Dempsey, R.C., Mathews, J.M., Henry G.W., Hall D.S. 1992, A&A, 265, 682
Ferriz-Mas, A., Schüssler, M. 1993, Geophys. Astrophys. Fluid Dyn., 72, 209
Ferriz-Mas, A., Schüssler, M. 1994, ApJ, 433, 852
Ferriz-Mas, A., Schüssler, M. 1996, Geophys. Astrophys. Fluid Dyn., , in press
Ferriz-Mas, A., Schmitt, D., Schüssler, M. 1994, A&A, 289, 949
Hall, D.S. 1990, in The Sun and Cool Stars: Activity, Magnetism, Dynamos, I. Tuominen, D. Moss, G. Rüdiger (Eds.), Springer, HeidelbergIAU Coll., 130, p. 353
Kitchatinov, L.L., Rüdiger, G. 1995, A&A, 299, 446
Moreno-Insertis F., 1983, A&A, 122, 241
Moreno-Insertis F., 1992, in: Sunspots, Theory and Observations, J. H. Thomas and N. O. Weiss (eds.), Kluwer, Dordrecht, 385
Moreno-Insertis, F., Caligari, P., Schüssler, M. 1995, ApJ, 452, 894
Moreno-Insertis, F., Schüssler, M., Ferriz-Mas, A. 1992, A&A, 264, 686
Parker, E.N. 1975, ApJ, 198, 205
Proctor, M. R. E., Weiss, N. O. 1982, Rep. Progr. Phys. 45, 1317
Schaller G., Schaerer G., Meynet G., Maeder A. 1992, A&A Suppl. Ser. 96, 269
Schou, J., Christensen-Dalsgaard, J., Thompson, M.J. 1994, ApJ, 433, 389
Schüssler M. 1993, in: The Cosmic Dynamo, F. Krause, K.-H. Rädler, G. Rüdiger (eds.), IAU-Symp. No. 157, Kluwer, Dordrecht, 27
Schüssler M. 1996, in: Solar and Astrophysical Magnetohydrodynamic Flows, K. Tsinganos (ed.), NATO ASI, Kluwer, Dordrecht, in press
Schüssler, M., Caligari, P., Ferriz Mas, A., Moreno-Insertis, F. 1994, A&A, 281, L69
Schüssler, M., Caligari, P., Ferriz Mas, A., Solanki, S.K., Stix, M. 1996, A&A, submitted
Schüssler, M., Caligari, P., Ferriz Mas, A., Solanki, S.K., Schaerer, D. 1996, in preparation
Schüssler, M., Solanki, S.K. 1992, A&A, 264, L13
Shaviv, G., Salpeter, E.E. 1973, ApJ, 184, 191
Skaley D., Stix M. 1991, A&A, 241, 227
Spiegel E.A., Weiss N.O. 1980, Nature, 287, 616
Spruit H.C. 1981, A&A, 102, 129
Spruit, H.C., van Ballegooijen, A.A. 1982, A&A, 106, 58
Tomczyck, S., Schou, J., Thompson, M.J. 1995, ApJ, 448, L57
Vogt, S.S., Penrod, G.D. 1983, PASP, 95, 565
Zahn, J.P. 1991, A&A, 252, 179
Zwaan, C. 1992, in: Sunspots–Theory and Observations, eds. J. H. Thomas & N. O. Weiss (Dordrecht:Kluwer), 75
Zwaan, C., Harvey, K.L. 1994, in: Solar magnetic fields, eds. M. Schüssler & W. Schmidt, (Cambridge University Press), 27

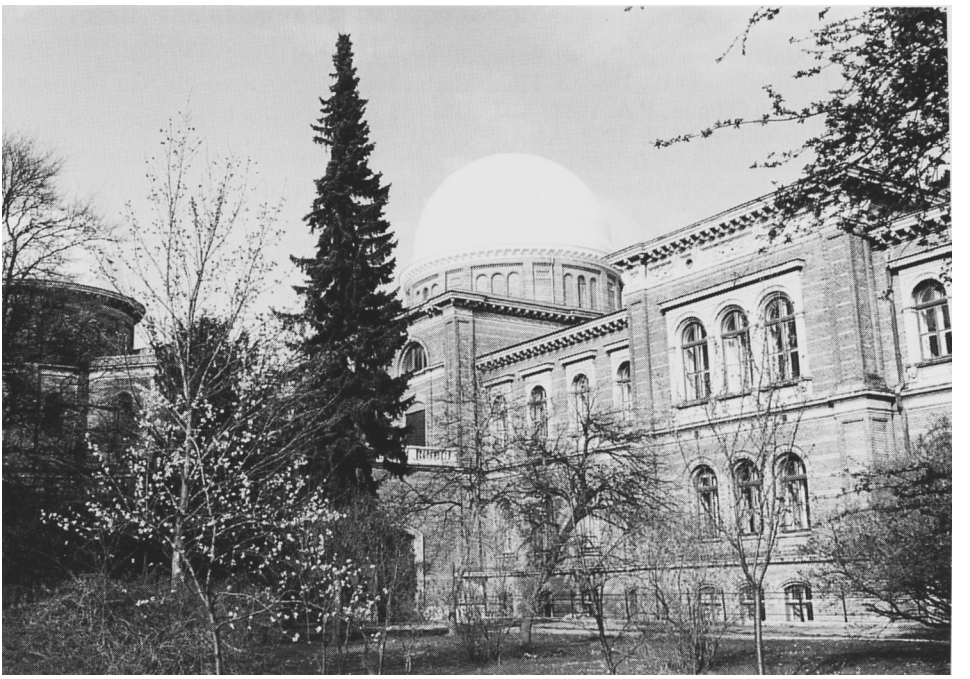

The Institute for Astronomy of the University of Vienna.

Welcome speach to "Der Kongreß tanzt" at the Institute for Astronomy (*right:* the district representative). Lots of waltz, food and drinks followed.

https://doi.org/10.1017/S0074180900083297 Published online by Cambridge University Press